IOPscience iopscience.iop.org

Home Search Collections Journals About Contact us My IOPscience

Field dependent creep characteristics in $Tl_2Ba_2CuO_6$ single crystals

This article has been downloaded from IOPscience. Please scroll down to see the full text article.

2004 J. Phys.: Condens. Matter 16 6727

(http://iopscience.iop.org/0953-8984/16/37/008)

View the table of contents for this issue, or go to the journal homepage for more

Download details:
IP Address: 129.252.86.83
The article was downloaded on 27/05/2010 at 17:32

Please note that terms and conditions apply.

INSTITUTE OF PHYSICS PUBLISHING JOURNAL OF PHYSICS: CONDENSED MATTER

J. Phys.: Condens. Matter **16** (2004) 6727–6736 PII: S0953-8984(04)81222-0

Field dependent creep characteristics in $Tl_2Ba_2CuO_6$ single crystals

P Chowdhury, Heon-Jung Kim, S K Gupta and Sung-Ik Lee

National Creative Research Initiative Center for Superconductivity and Department of Physics, Pohang University of Science and Technology, Pohang 790-784, Republic of Korea

Received 25 May 2004, in final form 29 July 2004
Published 3 September 2004
Online at stacks.iop.org/JPhysCM/16/6727
doi:10.1088/0953-8984/16/37/008

Abstract

The isothermal magnetization hysteresis loops were measured for $Tl_2Ba_2CuO_6$ (Tl-2201) single crystals by using a SQUID magnetometer and a micro Hall sensor. In the temperature window from 15 to 30 K, the Hall sensor measurements for $M(B)$ showed a second magnetization peak (SMP) at a peak field, B_{sp}, and an onset field, B_{on}. In this temperature region, the second peak appeared as a shoulder in the $M(H)$ plots when measured by using SQUID. At a temperature of 20 K, time relaxation measurements for the time interval of 1–10^4 s were carried out at different fields by using a Hall sensor. From these relaxation data, for both flux exit and entry, the activation barrier, U_0, and the creep exponent, μ, were separately calculated as a function of local field, B_z, by using the weak collective pinning theory. The variation of μ, and U_0 as a function B indicates that below the onset of the second peak field, B_{on}, the creep mechanism is an elastic process, but above it, a gradual transition to plastic creep takes place. At higher fields, μ and U_0 reduce sharply. This has been interpreted as a smooth transition to a 2D collective pinning state. These results are compared with that obtained in a double layer Tl compound, $Tl_2Ba_2CaCu_2O_8$ (Tl-2212), as well as other high-T_c materials.

The appearance of the fishtail or second magnetization peak (SMP) in isothermal magnetization curves at an intermediate field, H_{sp}, is a common feature and has been observed in most of the high temperature superconductors (HTSCs) [1–5]. The understanding of the mechanism leading to the origin of the SMP has been the subject of both theoretical and experimental investigations. It is well established that the onset of the SMP at a field of H_{on} in some high-T_c materials indicates a vortex phase transition from a weakly pinned vortex lattice to a strong pinned disordered vortex phase [1, 6], and theoretically this phase transition is described by a competition between the pinning and the elastic energies [7, 8]. However, several phenomena related to the fishtail effect are still not clear. For example, as the temperature is lowered below 20 K, this feature disappears altogether and appears again in longer timescales [9].

 © 2004 IOP Publishing Ltd Printed in the UK

Long-time magnetic relaxation measurements on an isothermal magnetization curve were found to be a useful tool to study the precise characteristics of vortex phases and phase boundaries at different fields. Extensive studies on field dependent magnetic relaxation have been carried out on $YBa_2Cu_3O_{6+y}$ (YBCO) [2, 3], pure $Bi_2Sr_2CaCu_2O_{8+y}$ (BSCCO) [10–12], Pb-doped BSCCO [4], and $Tl_2Ba_2CaCu_2O_8$ (Tl-2212) [5] single crystals by several groups. In these reports, the creep phenomenon for fields below H_{sp} was well explained based on weak collective pinning theory, and above it, the existence of dislocation-mediated plastic creep was observed, and the crossover from elastic to plastic creep was shown to be the origin of the second peak [2–4, 10, 11].

Among copper-based HTSCs, Tl-based compounds in single crystalline form were not studied extensively because of the high toxicity and volatility of thallium oxides. Recently, we have reported the magnetic properties measured on high-quality single crystals of a double layer Tl compound (Tl-2212) by using both a SQUID magnetometer and a Hall sensor [13, 14] and the results were found to be comparable with those observed in other high-T_c materials. However, recently there is much interest in the normal and mixed state of the monolayer Tl compound ($Tl_2Ba_2CuO_6$ (Tl-2201)) [15, 16], because in this compound, the critical superconducting transition temperature T_c can be varied from 90 K to ∼5 K by changing the oxygen doping. Since it has a T_c close to Tl-2212 ($T_c \sim 105$ K), it will be very interesting to compare the vortex creep characteristics with that obtained in Tl-2212 [5]. There are few reports on the SMP on Tl-2201 single crystals. In a report by Zuo *et al* [17] on Tl-2201 single crystal, it was observed that a dimensional crossover from 3D to 2D is responsible for the peak effect. In another report, Xu *et al* [18] found that the second peak field was independent of the oxygen defect concentration. A local field profile measured by using a Hall probe array was reported by Anders *et al* [19], where they observed that at the second peak field, the field gradient in the bulk of the crystal is maximum and the field independent relaxation rate was suggested to indicate the static origin of the second peak, which is contradictory to the observation made in BSCCO [20]. In BSCCO, the dynamic origin of the second peak was reported as it disappears on short timescales. Moreover, B_{sp} was observed to drift with time to lower fields [6, 5, 21]. Therefore, in this report, an extensive study on field dependent creep characteristics for a wider field range was investigated through long-time relaxation measurements to understand the origin of the second peak and the nature of the vortices in different field regions.

In this study, the isothermal magnetization curves of a high-quality Tl-2201 single crystal were measured by using a superconducting quantum interference device (SQUID) magnetometer and a micro Hall sensor. The SQUID measurements, carried out on an optimally doped sample ($T_c = 88$ K), showed a shoulder-like shape in the $M(H)$ plots obtained in the temperature range 15–30 K. A pronounced SMP was observed in the same temperature region when measurements were carried out using a micro Hall sensor. As the integration time for a commercial SQUID is larger than several tens of seconds, we have used a Hall sensor for studying the time dependent relaxation in a wide field region at a temperature 20 K. Using these relaxation data, the creep characteristics for Tl-2201 single crystals were evaluated. The results are also compared with the data measured on overdoped Tl-2201 single crystals.

Single crystals of $Tl_2Ba_2CuO_{6+\delta}$ were grown by the self-flux method, following a two-step procedure. In the first step, a 10 g polycrystalline pellet of Tl-2201 was made via solid state reaction from high-purity (99%) powders of Tl_2O_3, BaO, and CuO by calcining at 850 °C for 15 min in a preheated vertical furnace. In the second step, this pellet was reground and mixed with additional 10% CuO and 15% Tl_2O_3 by weight. Excess Tl_2O_3 was added to compensate for loss during the crystal growth, while the additional CuO acts as a flux. The mixture in the form of pellet was packed into a 30 ml conically shaped crucible and then it was sealed tightly by a another cylindrically shaped crucible. The whole arrangement was put into a preheated

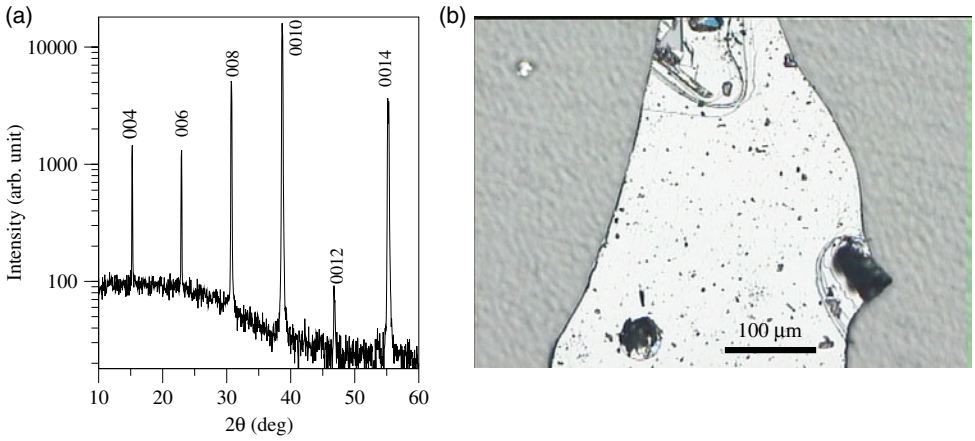

Figure 1. (a) X-ray diffraction pattern of a Tl-2201 single crystal measured by using a 4-circle goniometer. (b) Optical microscope image of a Tl-2201 single crystal.

(This figure is in colour only in the electronic version)

vertical furnace at 930 °C. After 30 min it was cooled to 870 °C in 10–15 h, then allowed to cool freely to room temperature. The crystal growth was performed in air. Thin platelet-type crystals having areas up to $\sim$1 mm^2 and very shiny surfaces were extracted mechanically from the solidified flux after crashing the crucible. In this two-step method, crystals of better surface quality as well as bigger size were obtained in comparison to the one-step method [22], particularly when a small amount of charge (<10 g) was used for growth.

To investigate the structural quality, x-ray diffraction (XRD) patterns was taken by using a 4-circle goniometer equipped with a primary monochromator (Cu Kα). The x-ray study showed very sharp reflections of 00l peaks with $c \sim 23.2$ Å that are characteristic of the 2201 structure as shown in figure 1(a) [16]. The crystals observed by using a polarizing optical microscope had very flat and shiny surfaces, as shown for a typical crystal in figure 1(b).

A crystal with dimensions 600 $\times$ 300 $\times$ 30 μm^3 was chosen to perform the extensive magnetization measurements. As shown in the inset of figure 2, the $M(T)$ measurement at a field of 10 G shows a very sharp transition at $T_c = 88.0$ K with $\Delta T_c \sim 2$ K. Initially, magnetic hysteresis loops, $M(H)$, at different temperatures (5–80 K) were measured by using a SQUID magnetometer with external magnetic field applied parallel to the c-axis. Figure 2 shows typical results obtained in the temperature range of 20–80 K. The $M(H)$ loops were recorded with increasing and decreasing fields (in steps) with the most rapid way possible in our technique. After measurements of the hysteresis loop at one temperature, the sample was heated to $T > T_c$ and cooled down to the next set temperature in zero field. The $M(H)$ loops did not show a pronounced second peak feature as observed in Tl-2212 single crystals [14], but at low temperatures ($T < 30$ K), they appear to have a shoulder-like shape. As discussed later, measurements using a Hall sensor show that this signature indicates the second anomalous magnetization peak in the $M(H)$ loop. A clear peak in the SQUID measurements is not obtained, as these measurements are averages over regions of different local inductions across the sample, and because of the sample's shape, square or rectangular blocks, edge effects cannot be neglected. For that reason, detailed hysteresis and magnetic relaxation measurements were performed on the same sample by using a Hall sensor.

For the local magnetization measurements, an InSb Hall sensor with an active area of 100 $\times$ 100 μm^2 and a resolution of 0.46 μV G^{-1} was attached at the centre of the crystal.

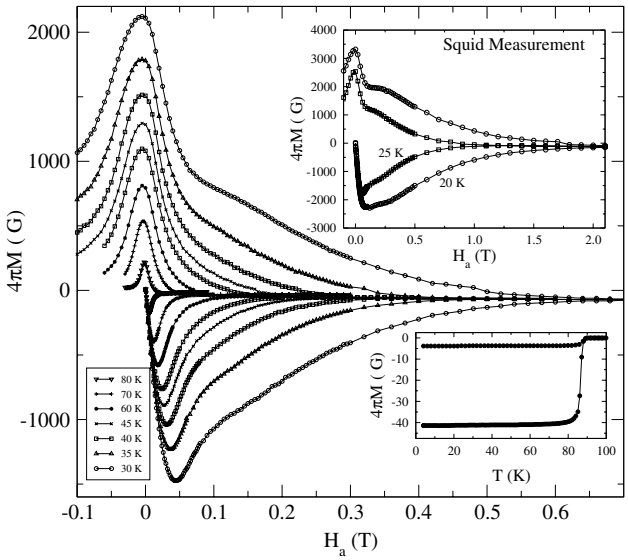

Figure 2. Field dependent magnetization, $M(H)$, measured using a SQUID magnetometer at different temperatures. The inset at the right upper corner shows $M(H)$ measured at temperatures 20 and 25 K. The inset at the lower right corner shows the $M(T)$ curve measured at a field of 10 G.

Measurements were performed by using a Maglab2000 (Oxford) system with magnetic fields up to 7 T applied parallel to the crystal c-axis by using a superconducting magnet. During measurements, the temperature was controlled with an accuracy of 5 mK. The local magnetization was defined as the difference between the z-component of the magnetic field measured by using the Hall sensor, B_z and the applied field, H_a. The local $M(B)$ loops measured for temperatures between 5 and 40 K are shown in figure 3. All the loops were measured with a ramp rate 10 G s^{-1} and at $t = 10$ s after ramping the field to the set value. In the temperature range 15–30 K, a second magnetization peak at a field of B_{sp} was observed in the $M(H)$ loop. As a pronounced second peak was observed at $T = 20$ K, we have also performed relaxation measurements at this temperature for different magnetic fields. During each set of relaxation measurement, the sample was first cooled down from 110 K (above T_c) to 20 K in zero field. For the ascending branch, after ramping the field with a constant sweep rate 10 G s^{-1} to the set field (above the full penetration field, $B_p \sim 950$ G), the magnetization data were recorded from 1 to 10 000 s. For the descending branch, the field was ramped to a field higher than 3 T and then set to the target field with the same sweep rate as mentioned above. For fields below B_p, the relaxation data corresponding to the ascending branch were measured at third quarter when the field was reversed in direction.

Figure 4 presents the relaxation data measured using a Hall sensor at $T = 20$ K, along with the $M(B)$ hysteresis loop measured at this temperature. For the relaxation measurement, the local field, B_z, was recorded as a function of time for fixed external field, H_a and $M(t) = B_z(t) - H_a$ was calculated. As the local field reduces with time, the value of B obtained from the $M(B)$ loop corresponding to that value of H_a was used to cite the relaxation data. From this figure it is seen that the envelope of the relaxation data measured at short times follows the $M(B)$ curve with a clearly defined second peak, but at longer times it changes to a shoulder-like shape. For analysis of the relaxation of the irreversible magnetization we need to subtract the reversible magnetization, M_{rev}, from the measured $M(t)$. Therefore, M_{rev} as

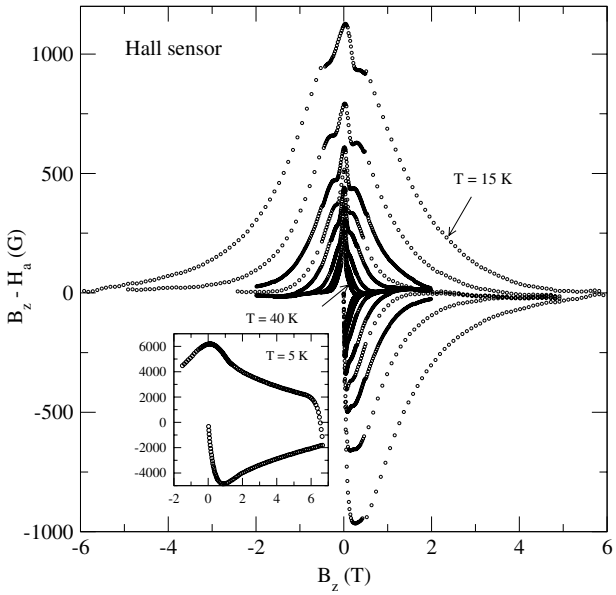

Figure 3. Field dependent magnetization, $M(B)$, measured using a Hall sensor at temperatures 15, 17.5, 20, 22.5, 25, 30, 35, and 40 K respectively. The inset shows $M(B)$ measured at $T = 5$ K.

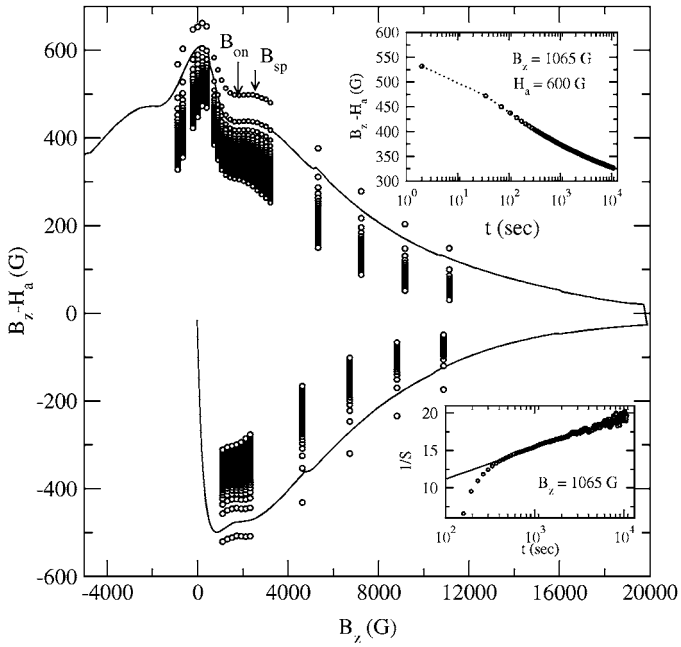

Figure 4. Field dependent local magnetization and magnetic relaxation measured using a Hall sensor at a temperature of $T = 20$ K. Here $M(B)$ measurements were performed at $t = 10$ s after ramping the field to the target field. In the relaxation measurements, the first data correspond to $t = 1$ s. The onset of the second magnetization, $B_{\rm on}$, and second magnetization peak field, $B_{\rm sp}$ are shown by arrow head lines. The inset at the upper right corner shows the variation in the irreversible component of the local magnetization with time for flux exit. The inset at the lower right corner shows the variation of $1/S$ versus $\ln(t)$. The slope at longer times gives the creep exponent μ.

a function of B_z was calculated from the $M(B)$ hysteresis loop measured at 20 K. Using the nonrelaxing $M_{\rm rev}$ corresponding to the local field, B_z, the irreversible magnetization $M_{\rm irr}(t) = M_{\pm}(t) \mp M_{\rm rev}$ was calculated for both flux entry and exit. Here, $M_{+}(t)$ and $M_{-}(t)$ are the measured local magnetization for flux entry and exit respectively. A typical behaviour of relaxation of irreversible magnetization determined for $H_{\rm a} = 600$ G and local field $B_z \sim 1065$ G is shown in the inset at the upper right corner of figure 4. A non-logarithmic behaviour for the local irreversible magnetization with respect to time t is seen. Therefore, the Anderson–Kim model [23] cannot be applied to analyse this data.

We interpret these relaxation data using predictions of the weak collective pinning theory, where the activation energy $U(j)$ and $M_{\rm irr}(t)$ ($\propto j$) for $j \ll j_{\rm c}$ are given by [24–26]

$$U(j) = U_0(B)\left(\frac{j_{\rm c}}{j}\right)^{\mu}, \tag{1}$$

$$M_{\rm irr}(t) = M_{\rm irr}(0)\left[\frac{k_{\rm B}T}{U_0}\ln(t/t_0)\right]^{-1/\mu}. \tag{2}$$

Here $U_0(B)$ is the collective pinning barrier, $j_{\rm c}$ is the critical current density, and t_0 is some attempt time for hopping of the vortex bundle. The exponent μ helps to identify various collective creep regions and depends on the applied magnetic fields and current. For a three-dimensional vortex system, $\mu = 1/7$ corresponds to the single vortex creep region expected at low fields and high currents, $\mu = 3/2$ to the small bundle creep region at intermediate currents and fields, $\mu = 1$ to the intermediate bundle region, and $\mu = 7/9$ to the large vortex bundle creep region expected at low currents and high fields. Using equations (1) and (2), the normalized creep rate may be written as $S = |{\rm d}\ln M_{\rm irr}/{\rm d}\ln t| = 1/\mu\ln(t/t_0)$. The slope of $1/S$ versus $\ln(t)$ is expected to yield the value of the exponent μ. However, as shown in the inset of figure 4 (lower right corner), there is a change in slope at the initial stage ($t < 400$ s) of the relaxation. This clearly indicates that equation (2) cannot be fitted to the experimental observed data for the whole time window by using a single μ value. Deviations for $t < 400$ s may arise due to transient effects after changing the field. Therefore, we have used the data for the time window of 400–10 000 s for determination of both U_0 and μ as a function of B_z for both flux exit and entry. Here, the value of t_0 was fixed to 10^{-3} s as reported for BSCCO single crystals [27].

The variation of μ with B_z is shown in figure 5(a) for both flux exit and entry. For a comparison, the $M(B)$ hysteresis loop for flux exit is also shown by using a solid line in this figure. It is seen that μ falls very sharply from a value of $\sim$1.7 at low fields to 1 at local field $B_z \sim B_{\rm p}$; however, a large difference in magnitude of μ between flux exit and flux entry was observed. With further increasing fields, μ increases, has a peak at a field $B_z^* \sim B_{\rm on}$, and then drops sharply to lower values. A comparison of the magnitude of μ with weak collective pinning theory indicates the existence of a small bundle region for fields below $B_z < \sim B_{\rm sp}$. Even close to the SMP region, the change in magnitude of μ is very small and does not signify any crossover in the creep mechanism. However, above $B_{\rm sp}$, μ drops sharply with increasing fields and reaches 0.4 for fields close to 1.1 T. Within the 3D collective pinning theory, this low value of μ indicates a transition towards to single vortex pinning ($\mu = 1/7$), which is not expected for high fields. Therefore, the results at high fields are in disagreement with 3D collective pinning theory, indicating another creep mechanism. This will be discussed later. In earlier studies, carried out in YBCO [2, 28] and LSCO [29] single crystals, for fields greater than full penetration field, $B_{\rm p}$, μ increases from 1 to 2 for $B < B_{\rm sp}$ and then decreases continuously towards zero at higher fields. Sometimes negative μ values have been observed at high fields. In our earlier report on Tl-2212 single crystals [5] as well as Pb-doped single crystals [4], μ was found to increase with field for fields less than B^* (lying between $B_{\rm on}$ and $B_{\rm sp}$)

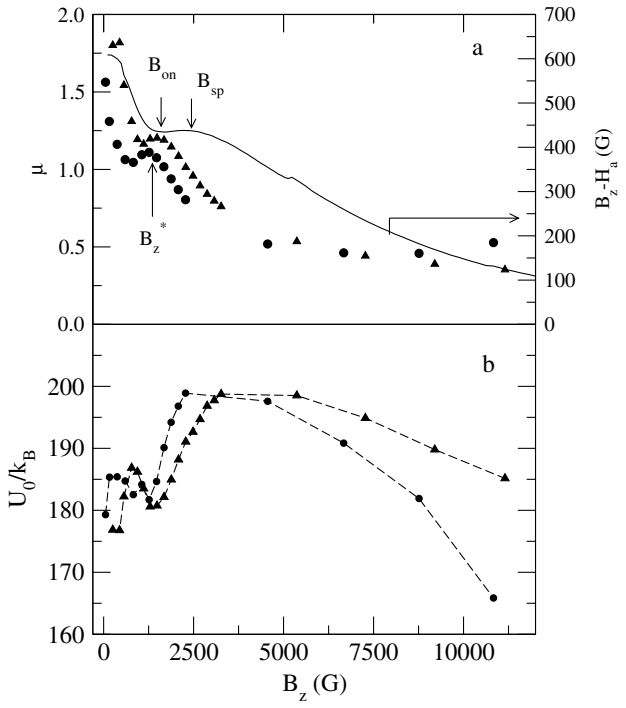

Figure 5. (a) The variation of creep exponent $\mu(B)$ along with the $M(B)$ hysteresis loop for flux exit at $T = 20$ K is shown. (b) This presents the variation of $U_0(B)$ at this temperature.

and then to reduce with further increasing fields. So, a comparison with some of these reports [2, 5, 28] suggests that the creep mechanism is controlled by an elastic creep process for fields less than B_{sp}, and above it, the sharp decrease in μ suggests another creep mechanism. We will now discuss the field dependence of U_0 to further understand the creep mechanism.

The variation of U_0 with B_z is shown in figure 5(b) in the lower panel. As with μ, a large difference between flux exit and entry was observed for fields less than $\sim B_p$, and $U_0(B)$ changes in non-monotonic fashion. This large difference is attributed due to the complicated field profile below the full penetration field, B_p [30]. In this region, the critical state model can introduce a error in calculating the true value of j_c, which causes large errors in calculating the correct magnitude of the physical quantities as well as the field dependences of them. A sharp increase of $U_0(B)$ was observed between B_{on} and $\sim B_{sp}$. Above B_{sp}, U_0 falls very sharply, but does not obey any power-law behaviour as reported in other high-T_c materials [2, 4, 28].

In the intermediate region, i.e., $B_p < B_z < B_{sp}$, the behaviour is somehow complicated. For fields from B_p to B_{on}, μ increases, whereas $U_0(B)$ decreases. This decrease of U_0 for fields less than B_{on} could be compared with that observed in LSCO [29] and Pd-doped BSCCO [4] single crystals. According to weak collective pinning theory, the activation energy increases with increasing bundle size. As in this region, an increment of μ suggests a decreases in bundle size, which results in a decrease of the activation energy. However, above B_{on} ($B_{on} < B_z < B_{sp}$), a sharp increase of the activation energy was observed. This can be understood in the following way. The onset of the magnetization, B_{on}, is believed to result from a competition between the elastic and the pinning energies. Therefore at $B \simeq B_{on}$, it is possible for the elastic energy to become comparable to the pinning energy and for vortex

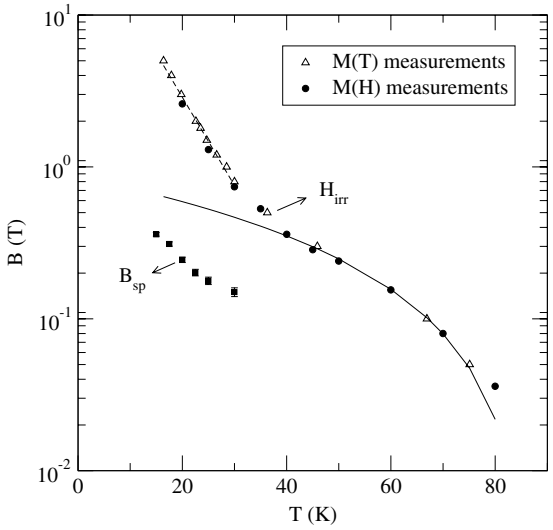

Figure 6. The variation of $H_{\rm irr}$ obtained from $M(T)$ and $M(H)$ measurements with temperature is shown. The second peak field, $B_{\rm sp}$, as a function of T is also shown in this figure.

interaction with pinning centres to result in an entangled solid, because entangled vortices adapt more efficiently to the pinning landscape induced by point disorder. Due to such long wavelength entanglement or twisting of vortex lattices, pinning efficiency is enhanced, which results in a sharp increase in the activation energy. With further increasing fields, say above $B_{\rm sp}$, more and more dislocations proliferate, vortex crossing angles will become large, and pinning efficiency decreases.

Above $B_{\rm sp}$, $U_0(B)$ was observed to follow a negative power-law behaviour in some of the earlier studies. The value of the power exponent ν, obtained so far for fields $B > B_{\rm sp}$, lies between ~ -0.5 and -0.7 for YBCO [2], pure BSCCO [10], Pb-doped BSCCO [4], Tl-1212 [11], and $HgBa_2CuO_{4+\delta}$ (HBCO) [31]. In all of the above studies, the negative power law was explained by a dislocation-mediated plastic creep based on the proliferation of dislocations in the entangled vortex structures, as proposed by Abulafia *et al* [2]. For such a plastic creep, the zero current activation energy $U_{\rm pl}$ can be written as [32] $U_{\rm pl} = \epsilon\epsilon a_0$, where $a_0 = (\Phi_0/B)^{1/2}$ is the lattice constant, $\epsilon_0 = \Phi_0^2/4\pi\mu_0\lambda_{ab}^2(T)$, and ϵ is the anisotropy parameter. For a constant temperature, this equation leads to $U_{\rm pl} \propto B^{\nu}$, with $\nu = -1/2$. This negative exponent indicates, for a plastic creep mechanism, that $U_0(B)$ decreases with field. However, in our case, though $U_0(B)$ decreases with the field, no power-law behaviour was seen. The decrease in $U_0(B)$ can be understood using data on irreversible field discussed below.

The variation of irreversible field, $H_{\rm irr}$, as a function of temperature obtained from both $M(H)$ and $M(T)$ measurements is shown in figure 6. The variation of the second peak field, $B_{\rm sp}$, with temperature is also shown in this figure. It was observed that the SMP disappears for temperatures above $T \sim 35$ K, which can be correlated with the crossover temperature, $T_{\rm cr} \sim 35$ K, of the irreversibility line, $H_{\rm irr}(T)$. For $T > T_{\rm cr}$, the vortex displacement is dominated by thermal fluctuations and is consistent with the Lindemann melting criterion. Therefore, $H_{\rm irr}$ can be interpreted as the melting line of the vortex lattice given by $H_{\rm m} = A(1 - T/T_{\rm c})^m$ with $m = 3/2$. In our case, we find $m = 1.46$ very close to $m = 3/2$, and the fit is shown by a solid line in figure 6. For $T < T_{\rm cr}$, $H_{\rm irr}(T)$ follows an exponential behaviour as $H_{\rm irr} = H_{\rm irr}(0)\exp(-2T/T_0)$ with $H_{\rm irr}(0) = 41.3$ T, an indication of thermally

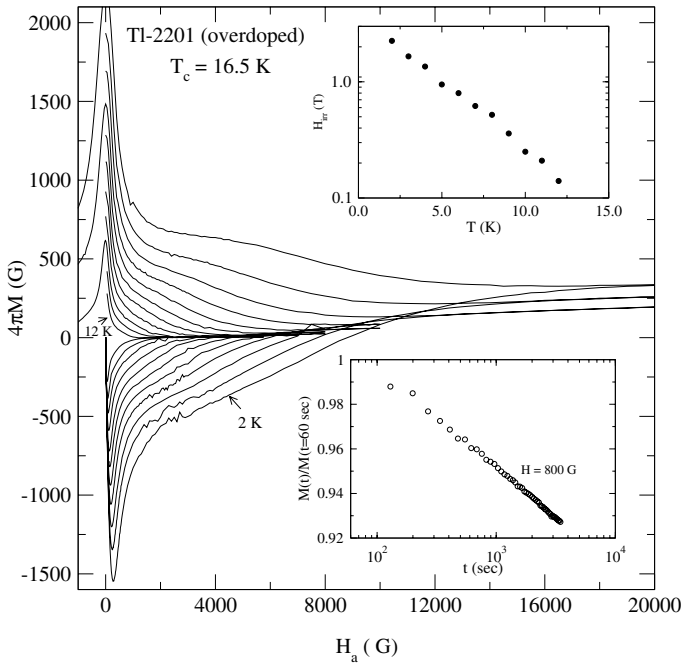

Figure 7. Field dependent magnetization, $M(H)$, measured for an overdoped sample using a SQUID magnetometer in the temperature range 2–12 K with 1 K interval. At the upper right corner, the variation of $H_{\rm irr}$ obtained from $M(H)$ measurements with temperature is shown. The relaxation measured at a field of 800 G and $T = 4$ K is shown in the lower right corner in a semilogarithmic plot.

activated pancake vortices on surface barriers as proposed by Burlachkov *et al* [33]. The presence of the pancake vortices near the irreversibility line might indicate that vortices above $B_{\rm sp}$, with increasing fields, gradually evolve to a decoupled regime of 'superentangled' pancake vortices. According to 2D collective pinning theory, the values of μ are 7/4, 13/16, and 1/2 for small bundle, medium bundle, and large bundle vortices, respectively. Our experimental value of $\mu \sim 0.4$ at higher fields might indicate the existence of the 2D collective creep (large bundle) region.

For a comparison, both the magnetization and the relaxation measurements using a SQUID magnetometer on a Tl-2201 overdoped crystal were carried out. The critical transition temperature, $T_{\rm c}$, was 16.5 K with $\Delta T_{\rm c} \sim 2$ K. Measurements of isothermal $M(H)$ hysteresis loops carried out on this sample are shown in figure 7. No signature of the second magnetization peak was observed in the temperature range 2–12 K. Moreover, in this temperature range, the irreversibility line shows an exponential behaviour, as shown at the upper panel of this figure. Extensive measurements of field dependent (400–6000 G) relaxation were also carried out on this sample at $T = 4$ K. For all the applied fields, the magnetization data as a function of time were found to follow a logarithmic behaviour. The typical behaviour of $M(t)$ for a field of 800 G is shown at the lower panel of figure 7. In this figure, the linear variation of M with $\ln(t)$ implies the applicability of the Anderson–Kim [23] formula. These analyses yield a monotonic decrease of the activation energy U_0 as a function of field (not shown here) and do not indicate any 3D to 2D crossover as observed in the optimally doped sample.

In conclusion, we have investigated the flux creep mechanism for a wide field range at 20 K in high-quality Tl-2201 single crystals. It was shown that the relaxation data were fitted

well with equation (2), predicted by weak collective pinning theory. At very low field range ($<H_p$), a large discrepancy within a physical quantity between flux exit and flux entry was observed. In the field range between B_{on} and B_{sp} the elastic creep controls the flux dynamics, but above B_{sp}, as indicated by the irreversibility field, H_{irr}, a smooth crossover to 2D pancake vortices takes place.

Acknowledgments

This work was supported by the Ministry of Science and Technology of Korea through the Creative Research Initiative Program. This work was partially supported by the National Research Laboratory Program through the Korea Institute of Science and Technology, Evaluation and Planning.

References

[1] Avraham N, Khaykovich B, Myasoedov Y, Rappaport M, Shtrikman H, Feldman D E, Tamegai T, Kes P H, Li M, Konczykowski M, Beek K V D and Zeldov E 2001 *Nature* **411** 451
[2] Abulafia Y, Shaulov A, Wolfus Y, Prozorov R, Burlachkov L, Yeshurun Y, Majer D, Zeldov E, Wuhl H, Geshkenbein V B and Vinokur V M 1996 *Phys. Rev. Lett.* **77** 1596
[3] Giller D, Shaulov A, Prozorov R, Abulafia Y, Wolfus Y, Burlachkov L, Yeshurun Y, Zeldov E, Vinokur V M, Peng J L and Greene R L 1997 *Phys. Rev. Lett.* **79** 2542
[4] Sun Y P, Song W H, Du J J and Ku H C 2002 *Phys. Rev.* B **66** 104520
[5] Chowdhury P, Kim H-J, Kang W N, Zang D-J and Lee S-I 2003 *Phys. Rev.* B **68** 134413
Chowdhury P, Kim H-J, Kang W N, Zang D-J and Lee S-I 2004 *Phys. Rev.* B **69** 109901 (erratum)
[6] Giller D, Shaulov A, Yeshurun Y and Giapintzakis J 1999 *Phys. Rev.* B **60** 106
[7] Ertas D and Nelson D R 1996 *Physica* C **272** 79
[8] Vinokur V, Khaykovich B, Zeldov E, Konczykowski M, Doyle R A and Kes P H 1998 *Physica* C **295** 209
[9] Li S and Wen H-H 2002 *Phys. Rev.* B **65** 214515
[10] Miu L, Cimpoiasu E, Stein T and Almasan C C 2000 *Physica* C **334** 1
[11] Aouaroun T, Hardy V and Simon Ch 1998 *Physica* C **294** 42
[12] Kim D H, Lee T W, Lee C W, Ha D H and Shim S Y 2002 *Physica* C **383** 23
[13] Chowdhury P, Kim H-J, Jo I-S and Lee S-I 2002 *Phys. Rev.* B **66** 184509
[14] Chowdhury P, Kim H-J, Jo I-S and Lee S-I 2003 *Physica* C **384** 411
[15] Hussey N E, Abdel-jawad M, Carrington A, Mackenzie A P and Balicas L 2003 *Nature* **425** 814
[16] Kim H-J, Chowdhury P, Gupta S K, Dan N H and Lee S-I 2004 *Phys. Rev.* B at press
[17] Zuo F, Khizroev S, Alexandrakis G C and Kopylov V N 1995 *Phys. Rev.* B **52** R755
[18] Xu M, Li T W, Hinks D G, Crabtree G W, Jaeger H M and Aoki H 1999 *Phys. Rev.* B **59** 13632
[19] Anders S, Xu M, Jaeger H M, Li T W and Hinks D G 1999 *Phys. Rev.* B **59** 13635
[20] Anders S, Parthasarathy R, Jaeger H M, Guptasarma P, Hinks D G and van Veen R 1998 *Phys. Rev.* B **58** 6639
[21] Radzyner Y, Shaulov A, Yeshurun Y, Felner I, Kishio K and Shimoyama J 2002 *Phys. Rev.* B **65** 100503
[22] Ozyuzer L, Yusof Z, Zasadzinski J F, Li T-W, Hinks D G and Gray K E 1999 *Physica* C **320** 9
[23] Anderson P W and Kim Y B 1964 *Rev. Mod. Phys.* **36** 39
[24] Blatter G, Feigel'man M V, Geshkenbein V B, Larkin A I and Vinokur V M 1994 *Rev. Mod. Phys.* **66** 1125
[25] Larkin A I and Ovchinnikov Yu N 1979 *J. Low Temp. Phys.* **34** 409
[26] Vinokur V M, Kes P H and Koshelev A E 1990 *Physica* C **168** 29
[27] Niderost M, Suter A, Visani P, Mota A C and Blatter G 1996 *Phys. Rev.* B **53** 9286
[28] Küpfer H, Gordeev S N, Jahn W, Kresse R, Meier-Hirmer R, Wolf T, Zhukov A A, Salama K and Lee D 1994 *Phys. Rev.* B **50** 7016
[29] Kodama Y, Oka K, Yamaguchi Y, Nishihara Y and Kajimura K 1997 *Phys. Rev.* B **56** 6265
[30] Wiesinger H P, Sauerzopf F M and Weber H W 1992 *Physica* C **203** 121
[31] Pissas M, Stamopoulos D, Moraitakis E, Kallias G, Niarchos D and Charalambous M 1999 *Phys. Rev.* B **59** 12121
[32] Geshkenbein V B, Larkin A I, Feigel'man M V and Vinokur M V 1989 *Physica* C **162–164** 239
[33] Burlachkov L, Geshkenbein V B, Koshelev A E, Larkin A I and Vinokur V M 1994 *Phys. Rev.* B **50** 16770